

Comparative study of glycerol diglycidyl ether/aliphatic amines networks

Ándres Felipe E.Pineda^a, F. González Garcia^{a*}, Bluma G. Soares^b, Alexandre Z. Simões^c,
Elson L. da Silva^d

^aInstituto de Física e Química, Universidade Federal de Itajubá, Ave BPS. No 1303, Pinheirinho, 37500-903, Itajubá, MG, Brazil

^bInstituto de Macromoléculas, Universidade Federal de Rio de Janeiro, Centro de Tecnologia, Bl J, Ilha do Fundão, 21945-970, Rio de Janeiro, RJ, Brazil.

^cFaculdade de Engenharia de Guaratinguetá, Universidade Estadual Paulista, Ave. Dr. Ariberto Pereira da Cunha No. 333, Guaratinguetá, 12516-410, SP, Brazil.

^dInstituto de Química, Universidade Estadual Paulista, Rua Francisco Degni No. 55, Quitandinha, 14800901, Araracuara, SP, Brasil.

*Corresponding Author Email: fili@unifei.edu.br

Sponsoring information:

This work was financially supported by the Brazilian research funding agencies FAPEMIG Process APQ. 00073-13 and CNPq; Project MCTI/Universal 14/2014, process No. 446735/2014-0.

Abstract:

In this study, dynamic-mechanical analysis, mechanic properties, adhesive strength, and water absorption of networks based on glycerol diglycidyl ether cured with aliphatic diamines were studied. Dynamical-mechanical spectra were used to study both α and β relaxations. The mechanical properties were evaluated by tensile, flexural and compression testing. The adhesive strength was evaluated in terms single lap-shear using 316L stainless steel as the adherend. The water absorption was evaluated by immersion at $(37 \pm 0.2)^\circ\text{C}$. The fracture mechanisms of the adhesive joints were determined by optical microscopy. The polymers based on cyclic diamine showed relative high- T_g , high tensile and flexural modulus and compression yield stress, the best adhesive strength, and greater participation of cohesive fracture mechanisms. In addition, the increases molecular rigidity in the diamine decreases the water absorption.

Keywords: 316L stainless steel; epoxy/amine networks; mechanical properties; adhesive strength; water absorption.

1. INTRODUCTION

Epoxy polymers are one of the most important classes of thermosetting materials and have wide use as adhesives. Formulations containing nanoclays, polyhedral oligomer silsesquioxanes, block copolymers, carbon nanotubes and so on are being continuously developed of matrices for composites materials. The study of the epoxy polymers is still of great interest by many researched (Pascault J.P. et al., 2010). Unfortunately, these materials have a drawback, being brittle and having poor resistance to crack propagation. This negative aspect is usually improved by changes of the crosslink density and/or flexibility of chain between crosslinks to act on the structure of the epoxy monomer (Cukierman S. et al., 1991, Morel, E. et al., 1989, Choy, I. et al., 1986) or of the diamine comonomer (González Garcia F. et al., 2010, Grillet A.C. et al., 1989, Varma I.F. et al., 1986, Delvigs P. et al., 1986). The better method to the control to the crosslink density is by using a mixture of a monoamine and primary diamine comonomer (Charlesworth J. et al., 1988, Won, Y.G. et al., 1990). Another possible way is by addition of modifiers such as; elastomers or thermoplastics (Abadyan M. et al., 2012, Tripathy R. et al., 2011, Khoee S. et al., 2010, Kuan H.C. et al., 2010, González Garcia F. et al., 2010, Maiez-Tribu S. et al., 2007).

The use of sterically hindered aliphatic or cycloaliphatic diamines comonomer as curing agent have long gel times which is a fascinating place for purposes of easy processing. For more than twenty years, much attention has been paid to the characterization of networks based on cycloaliphatic diamine such as methane diamine or isophorone diamine (IPD) (Won Y.G. et al., 1990, Mortarnal S. et al., 1989) and sterically hindered cycloaliphatic diamine such as 4,4'-diamino-3,3'-dimethyldicyclohexylmethane (3DCM) (Urbaczewski-Espuche E. et al., 1991). Also, another type of hardener based on sterically hindered aliphatic flexible diamines as such poly(oxypropylene diamine) backbone known by Jeffamines has been studied. The poly(oxypropylene diamine) are a polyether oligomers of different molecular weight terminated at each end with an amine primary group which a methyl group derived from the polyester, which corresponds to the poly(oxypropylene) structure. These compounds (e.g., D230, D2000, T403, etc.) have low viscosity and vapor pressure, and have been developed and achieved commercial success for many years. In addition, as curing agent for epoxy monomers, the polymers most exhibit toughness (Cai H. et al., 2008, Froimowicz P. et al., 2005, Fernandez-Nograro F. et al., 1996), and in most cases an improved in elongation at break and impact strength (Yan G. et al., 2007).

The glycerol diglycidyl ether (DGEG) as an epoxy monomer has a low viscosity at room temperature. These epoxy monomers was recently investigated for coating applications (Omrani A. et al., 2011 and 2013). The study of the networks based on this aliphatic epoxy prepolymer is very interesting because the cure with aliphatic diamines can be result in thermosetting materials with greater flexibility compared to the networks based on aromatic epoxy monomer (bisphenol A diglycidyl ether, DGEBA). In this way it is believed that the aliphatic epoxy polymers are more advantageous for cardiovascular applications, as for example for surface coating of coronary stents manufactured with 316L stainless steel, because our studies with *in vitro* biological properties indicate that the something aliphatic epoxy polymers are haemocompatible, no signs of cytotoxicity to Chinese hamster ovary cells and to MG63 osteoblasts-like cells (González Garcia F. et al., 2009, 2016 and 2017, Silva A. et al., 2016). However, for this application it's necessary to found a coating material with adequate mechanical properties, good adhesive strength, and low water absorption in physiological environment (37 °C).

Numerous studies have been published on the mechanical properties (Yan G. et al., 2007, González Garcia F. et al., 2009 and 2007, Crawford E.D. et al., 1999, Cook W.D. et al., 1988), adhesiveness (González Garcia F. et al., 2011, Hu X. et al., 2005, Lapique F. et al., 2002), water absorption (Colombini D. et al., 2002, Pineda A.F. et al., 2016), adhesive applications of epoxy formulations, for various metals, including stainless steel (De Morais, A.B. et al., 2007) and dynamical-mechanical properties (Fernandez-

Nograro, F. et al., 1996, Colombini, D. et al., 2002). However, to our knowledge we did not find a comparative study of the dynamical-mechanical analysis, mechanical properties and adhesive resistance for the 316L stainless steel substrate and water absorption in physiological environment (at 37 °C) of epoxy formulations from diglycidyl ether of bisphenol A (DGEBA) and glycerol diglycidyl ether (DGEG) cured with poly (oxypropylene diamine) (D230).

The aim of this work is an attempt to evaluate the effects chemical structure of the diamine on the thermal relaxation, mechanical properties, and adhesive strength on 316L stainless steel and water absorption in physiological environment (at 37 °C).

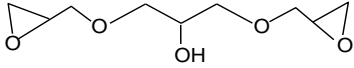
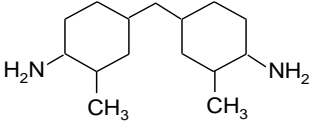
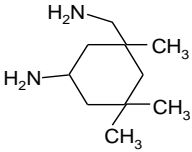
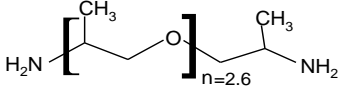
In order to maintain a linear structure in the aliphatic diamine, the poly(oxypropylene diamine) (D230) was chosen. The other aliphatic diamines were based on isophorone diamine (IPD) and 4,4'-diamino-3,3'-dimethyldicyclohexylmethane (3DCM), both having cyclic structures.

2. MATERIALS AND METHODS

2.1 Materials

Glycerol diglycidyl ether (DGEG) which epoxide equivalent weight of 143.0 g/eq as determined by acid titration was used as the epoxy monomer in all studied formulations. Three conventional diamine as curing agents, i.e. an aliphatic diamine, poly(oxypropylene diamine) (D230), and two cycloaliphatic diamines; isophorone diamine (IPD) and 4,4'-diamino-3,3'-dimethyldicyclohexylmethane (3DCM) having amine-hydrogen equivalent weights of 48.0, 42.6 and 59.6 g/eq, respectively, as determined by potentiometric titration in an aqueous medium (González Garcia F. et al., 2007) were used without purification. The chemical structures, suppliers, purities, molecular weights, and functionalities of the monomers are listed in Table 1. Reagent and solvents including (3-aminopropyl) trimethoxysilane (APTS, 97%, Sigma-Aldrich) and analytical-grade; acetone 99%, and ethanol 95% (Vetec, Brazil) were used as received. The medical-grade 316L stainless steel was the commercial VI 138 stainless steel (specialty alloy, ASTM – F138) from Villares Metals, Brazil.

Table 1. Structure and characteristics of the various monomers

| Monomers | Chemical Structure | Supplied | M g mol ⁻¹ | F |
|--|---|---------------------------------|--------------------------|---|
| Diglycidyl ether of glycerol (DGEG) |  | Sigma-Aldrich (technical grade) | 204.22 | 2 |
| 4,4'-Diamino-3,3'-dimethyldicyclohexylmethane (3DCM) |  | Aldrich (99.0%) | 238.41 | 4 |
| Isophorone diamine (IPD) |  | Aldrich (99.0%) | 170.30 | 4 |
| Poly(oxypropylene) diamine (D230) |  | Sigma-Aldrich Jeffamine D230 | ~230.00 | 4 |

M: Molecular weight, F: Functionality.

2.2 Preparations of the specimens

The specimens were prepared by carefully weighing of the monomers at stoichiometric amount (epoxy/amine hydrogen $e/a=1$). All mixtures were degassed at room temperature (25 °C) under magnetic stirring until a homogeneous liquid was obtained. The mixtures were poured in to a silicone mold, cured in forced-air oven at 60 °C for 4 h, and submitted to post-cure state at 180 °C, 160 °C and 130 °C during 2 h, for the formulations based on 3DCM, IPD and D230, respectively, then allowed to cool slowly to room temperature. Specimens for mechanical and water absorption testing were machined as plates or cylinders from the molded material, to reach the final required dimensions and improve the surface finish.

2.2 Preparations of lap shear specimens

The adhesive strength was evaluated for mechanical tests using single-lap shear joint. The geometry of adhesive joint is shown in Figure 1. The 316L stainless steel used was a commercial material from the Villares Metals (Brazil). In order to increase the adhesive properties, the metallic adherend surfaces were treated by ultrasonic cleaning in acetone at 45 °C for 5 min, dipped in acetone 45 °C for 5 min, and dried by dabbing with absorbent paper and a dry nitrogen flow. The metal plate surfaces were then chemically treated in a sulfochromic bath (97 % sulfuric acid and 3% potassium dichromate) at 60 °C for 10 min, rinsed with distilled water and blown dry with nitrogen gas. After the chemical treatment, the metal surfaces were silanized by a silane solution (APTS, 0.12 % v/v) in a mixture of ethanol and distilled water at 25%/75% (v/v), according to the methodology reported elsewhere (Chovelon J.M. et al., 1995). The specimens were stored in a glass dryer with silica gel until testing.

For the adhesive applications, specific metallic mold was designed for adhesive joint. The design of the mold allows control the exactly layer thickness. After surface treatment, metallic pieces were assembled for adhesive single-lap shear joint. The adhesive formulations were prepared as mentioned in the specimen preparation. The epoxy formulation was applied uniformly on both surfaces of the adherend with the sample introduced in the specific metallic molds. The applied contact pressure was kept constant, which allows obtaining specimens with uniform adhesive thickness, 0.2 ± 0.04 mm. The specimens in the molds were cured as mentioned in the specimen preparation. To reduce the deviation of the adhesive layer, respect to the tensile axis, chocks in the extremes of the specimens were used (see Fig. 1). These specimens were maintained at room temperature 22 ± 2 °C and relative humidity of 50 ± 5 % during 24 h before testing.

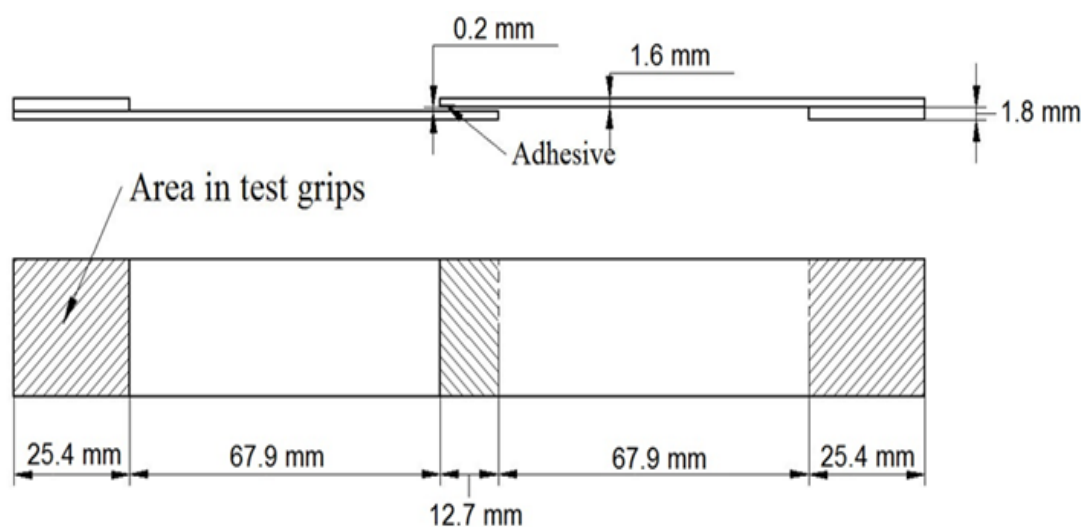


Fig. 1. Dimensions of the adhesives joints of single lap shear using 316L stainless steel adherend (measured in mm).

2.3 Testing of the adhesive specimens

The adhesive strength of the single-lap shear joints were performed on a DL2000 EMIC machine at a crosshead speed of 3 mm/min with a 0.5 kN load cell, according to ASTM D 1002 standard. The lap shear strength was expressed in MPa. The adhesion tests were carried out at 22 ± 2 °C and relative humidity of 50 ± 5 %. The average values were taken from at least eight specimens.

2.4 Differential scanning calorimetry measurements (DSC)

Differential scanning calorimetry measurements (DSC) were performed on a Shimadzu model DSC-60 under nitrogen purge. The samples 10 ± 2 mg were heated from -30 to 200 °C at a rate of 10 °C/min. The presence of residual heat (ΔH_R) was evaluated from the first scan. The samples were rapidly cooled at -30 °C and heated again at the same rate, to obtain the glass transition temperature (T_g). The T_g was taken as the temperature corresponding to the middle of the middle of heat capacity base-line change. The first scans of all samples showed that no residual heat appear indicating that no additional cure occurs.

2.5 Dynamic mechanical measurements (DMA)

The dynamic mechanical measurements (DMA) of the epoxy networks were performed on a dynamic mechanic analyzer Q800 (TA Instruments) using single cantilever-type clam. The experiments were carried out on prismatic samples of dimension equal to 2.5 mm in depth, 10 mm in width, and 2.5 mm in length. The α transition was studied between 30 and 190 °C at a heating rate of 2 °C/min and a frequency of 1 Hz in nitrogen atmosphere. The β relaxation was studied between -120 and 40 °C at a heating rate of 2 °C/min in a frequency range from 3.0×10^{-1} Hz to 3.0×10^1 Hz always in nitrogen atmosphere. The apparent activation energy $E_{a\beta}$ of the β relaxation was determined using an Arrhenius law on the maxima of the β peak (T_β). These experiments yield the storage modulus, E' the loss modulus, E'' and the damping factor, $\tan \delta$ (E''/E') was determined from the peak of the $\tan \delta$ curve.

$$\log v = E_{a\beta}/RT_\beta + \text{constant} \quad (1)$$

2.6 Tensile tests

Tensile tests were performed on a DL2000 EMIC machine at a crosshead speed of 3 mm/min with a 0.5 kN load cell, according to ASTM D638M. The Young's modulus E was computed from the linear part of the curve; yield strain and yield stress at break were also recorded. Condition the test specimens at 23 ± 2 °C and 50 ± 5 % relative humidity. The results were taken from an average of at least six specimens and the results averaged to obtain a mean value.

2.7 Flexural tests

The specimens were tested under flexural conditions. The mechanical tests were made using the same testing machine with specimen dimensions equal to 100 ± 0.1 mm x 10.0 ± 0.1 mm x 4.5 ± 0.1 mm according ASTM D790 standard. The values of flexural modulus, flexural stress, and flexural strain at break were determinates. All measurements were conducted in three-point bending and a fixed span length of 80 ± 0.1 mm at a speed of 5 mm/min. Measurements were performed for each specimens at 50 ± 5 % relative humidity at 23 ± 2 °C, and the report value were averaged from measurement of at least ten specimens. The specimens were tested to fracture and the flexural stress (σ_f), flexural strain (ε_f) and the flexural modulus (E_y) were calculated from the following equations:

$$\sigma_f = 3PL/2bd^2 \quad (2)$$

$$\varepsilon_f = 6Dd/L^2 \quad (3)$$

$$E_f = L^3m/4bd^3 \quad (4)$$

where: P is the load at the break or yield, b and d are the width and the thickness of the specimen respectively, L is the length between supports, d is the maximum deflection of the center of the beam and m is the slope of the tangent of the initial straight-line portion of the load-deflection curve.

2.8 Compression tests

Compression tests were made using the same testing machine under ASTM D695 protocol at 23 ± 2 °C with a 5 kN load cell at speed of 1 mm/mm. Cylindrical specimens 20.0 ± 0.2 mm long with, 10.0 ± 0.2 mm diameter were deformed in a compression ring between steel plates. The compressive yield strength (σ_c) and the compressive yield strain (ε_r) were determined. The reported values were average from measurement of at least ten specimens.

2.9 The failure mechanisms

The failure mechanisms of the different adhesive joints were determined by optical microscopy (Topcon) with imaging analysis software. The fracture surfaces were observed and recorded by optical microscopy. The images were transmitted by a video camera to a personal computer. The dark and clear regions were attributed to cohesive and adhesive failure, respectively. The percentage of cohesive failure was calculated as the quotient of the dark areas and the total area of the metal substrate multiplied by 100.

2.10 Water absorptions

Test specimens of (15.0 ± 0.2) mm x (10.0 ± 0.2) mm x (3.2 ± 0.2) mm were used for water absorption tests, following the recommendations of ASTM D570 standard of testing specimens of sheet materials. The samples were removed at regular intervals from a bath of distilled water (at 37.0 ± 0.2)°C, carefully wiped with a filter paper, and weighed on an analytical balance with a precision of ± 0.01 mg. Three specimens were used per each epoxy polymer. The mass water absorbed C_t (%) by the specimens was calculated with the following expression (Equation 1):

$$C_t(\%) = \left(\frac{w_t - w_0}{w_0} \right) * 100 \quad (5)$$

where: w_t is the mass of the specimens at time t , w_0 is the mass of the dry specimen. The average standard deviation corresponds to the value less than 0.05% on the C_t (%) scale.

3. RESULTS AND DISCUSSION

3.1 Dynamic mechanical measurements (DMA)

A typical plot of the storage modulus E' and $\tan \delta$, measured at 1Hz, as a function of temperature, is shown in Figure 2 for the DGEG/3DCM network. Three relaxations are observed:

- (i) a main transition, α in the high-temperature region, is associated with the glass transition;
- (ii) a secondary relaxation, β , below 0 °C;

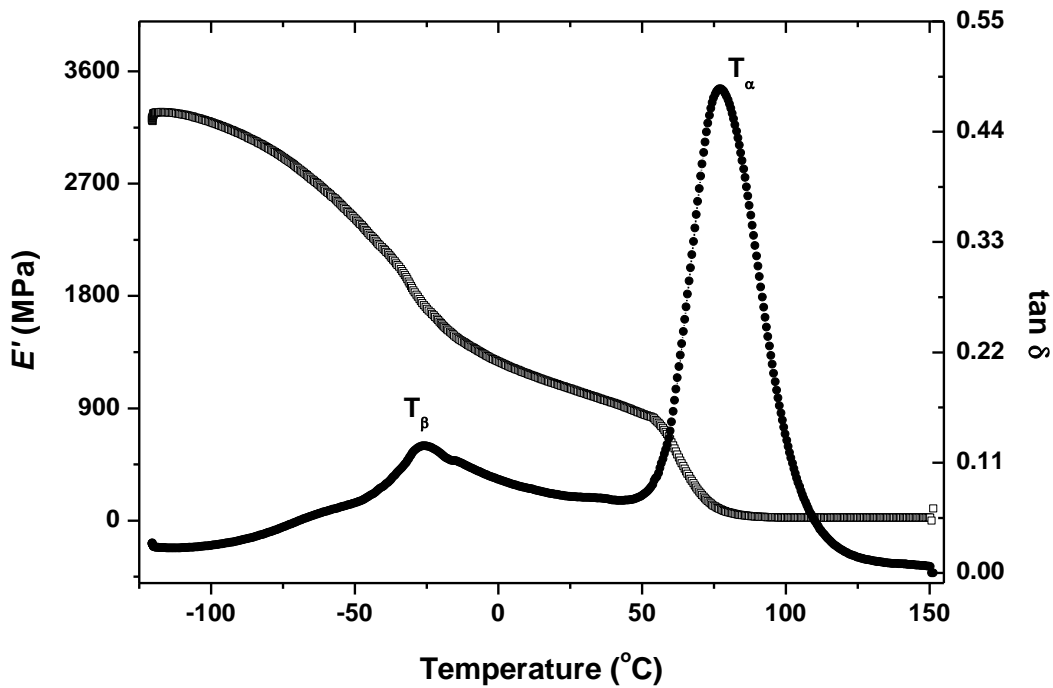


Fig. 2. Dynamical mechanical properties of the DGEG/3DCM network, measured at 1 Hz.

Table 2 gives the values of the mechanical relaxation T_{α} determined at the maximum of the loss peak and the intensity at this maximum ($\tan \delta$).

Table 2. Characteristics of the α relaxation at 1 Hz for the epoxy networks

| Epoxy Networks | T_{α} (°C) | $\tan \delta$ |
|----------------|-------------------|---------------|
| DGEG/3DCM | 76.4 | 0.49 |
| DGEG/IPD | 63.8 | 0.58 |
| DGEG/D230 | 25.4 | 0.98 |

T_{α} = temperature at the maximum, $\tan \delta$ = amplitude of the loss peak at its maximum.

The effect of different curing agents for the different epoxy networks on the $\tan \delta$ in the high-temperature region is shown in Figure 3.

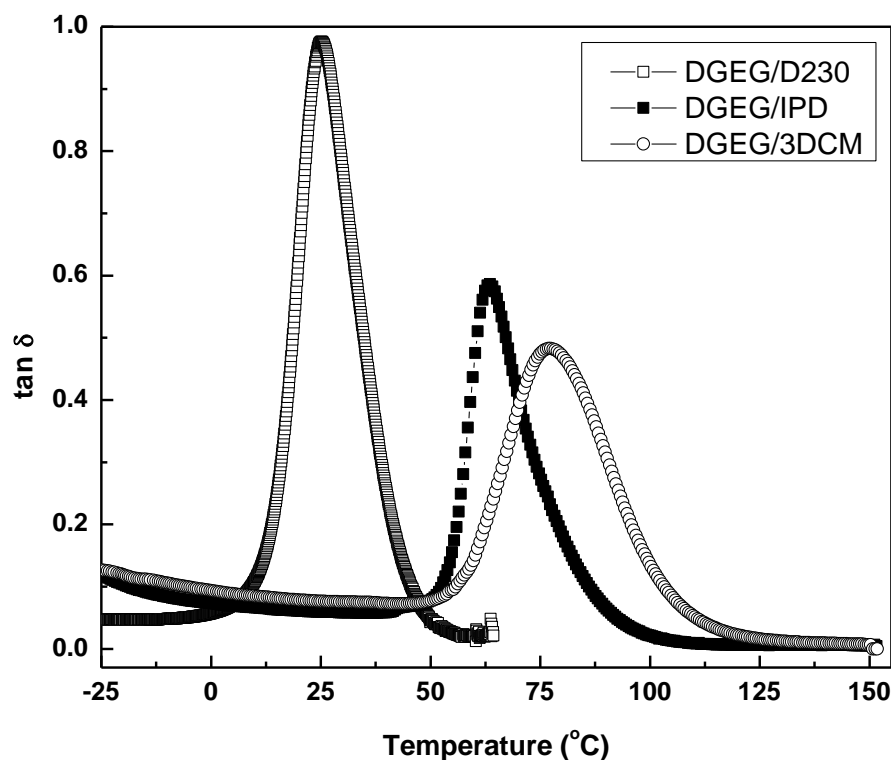


Fig. 3. Tan δ of the epoxy networks as a function of temperature at 1 Hz.

The differences between the shapes of the α peaks are related to the structure of the diamine as curing agent. The epoxy network based on 3DCM and IPD (cyclic diamines) present relative higher T_{α} and lower $\tan \delta$ values than that based on D230 as the curing agent, due to the increase in molecular rigidity of the systems cured with cyclic diamine.

From these results, it is possible to infer that the linear diamine D230 originates a more flexible network. This can be explained considering that the network formation involves an aliphatic epoxy monomer with a linear aliphatic amine comonomer, this with flexibility chain segments (see Table 1) and this structural segment provokes the formation of chains between two crosslinks with greater spacing, and consequently lower- T_g value as expected (Urbaczewski-Espuche E. et al., 1991, González Garcia F. et al., 2007, Pascault J.P. et al., 2001).

The β relaxation is related to the short molecular segment motion and depends on the chemical structure of the compounds (Ochi M. et al., 1987 and 1986). For epoxy/amine networks, most authors (Heux, L. et al., 1997, Struik L.C.E. 1987, Ochi M. et al., 1985) associate the β relaxation (between -80 °C and -40 °C) with motion contributions of diphenylpropane groups and glyceryl units:

Spectra for three epoxy networks are shown in Fig. 4 and their characteristics (T_{β} = temperature of $\tan \delta_{\max}$ and $E_{a\beta}$ = activation energy) are reported in Table 3.

The β relaxation in the cyclic diamine series 3DCM and IPD are similar, while in the linear diamine D230 the relaxation presents very low intensity and shifted to lower temperature. The apparent activation energy ($E_{a\beta}$) is related to the experimental molecular weight segment between the crosslinking points. It has been suggested that the $E_{a\beta}$ value decreases with increasing molecular weight of segment between

crosslinked points (Grillet A.C. et al., 1989, González Garcia F. et al., 2009). In Table 3 it can be observed that the $E_{a\beta}$ values for the linear and cyclic diamine series agree with expectations.

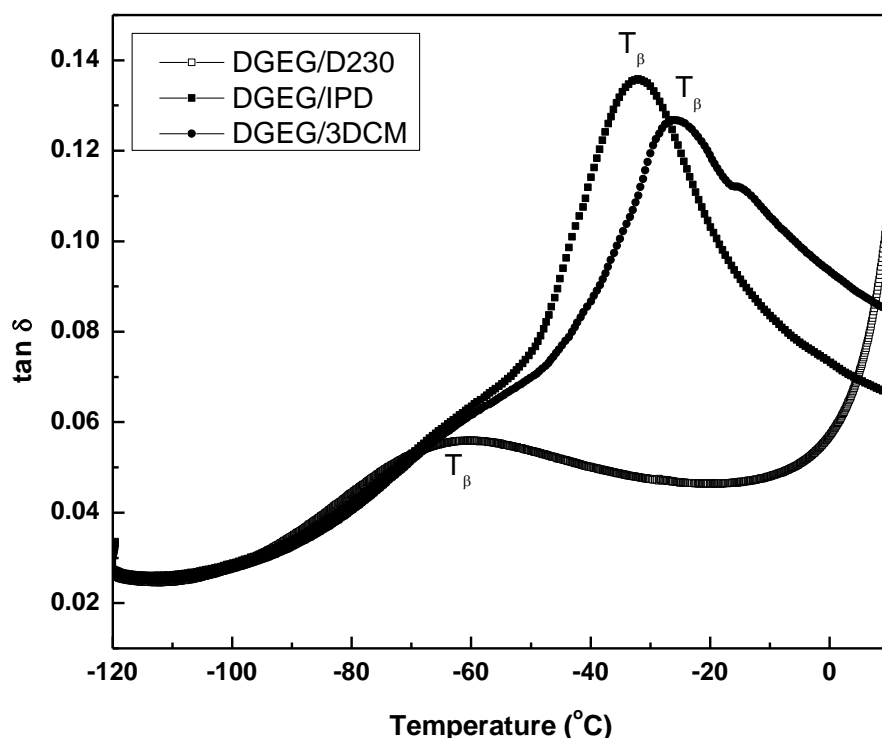


Fig. 4. β Relaxation for the various networks measured at 1 Hz.

Table 3. Characteristics of the β relaxation at 1 Hz

| Epoxy Networks | T_{β} (°C) | $E_{a\beta}$ (kJ mol ⁻¹) |
|----------------|------------------|--------------------------------------|
| DGEg/3DCM | -25.8 | 52 |
| DGEg/IPD | -32.0 | 54 |
| DGEg/D230 | -66.1 | 60 |

T_{β} = temperature at the maximum, $E_{a\beta}$ = activation energy.

3.2 Mechanical and adhesive properties

Tensile, flexural and compression tests were performed to evaluate the effects of the chemical structure of the comonomer on the mechanical properties of epoxy networks. As shown in Tables 4, 5 and 6 the T_g of the epoxy networks presents large influence on the mechanical behavior. The system cured with 3DCM or IPD (cyclic amines) present relative higher- T_g value, and better mechanical strength in terms of modulus and tensile, flexural or compression resistances that those observed for the system cured with D230. This is associated with the more molecular rigidity of the cyclic diamine series compared to a linear diamine. From these results, it is possible to infer that the diamine D230 originated a flexible material. This is in agreement with results in dynamical mechanical analysis and this behavior was only observed for this system (see Figure 5).

Table 4. Thermal and mechanical properties of the epoxy networks in tensile tests

| Epoxy Networks | $T_g(^{\circ}\text{C})$ | E (GPa) | σ (MPa) | ϵ (%) |
|----------------|-------------------------|------------------|------------------|------------------|
| DGEG/3DCM | 78.2 | 5.81 ± 0.37 | 56.12 ± 2.27 | 11.99 ± 0.52 |
| DGEG/IPD | 65.5 | 4.58 ± 0.88 | 49.12 ± 3.10 | 13.36 ± 0.21 |
| DGEG/D230 | 12.6 | 0.03 ± 0.002 | 2.81 ± 1.59 | 33.39 ± 7.88 |

E = Tensile modulus; σ , ϵ = tensile stress, strain at the maximum.

Table 5. Thermal and mechanical properties of the epoxy networks in flexural tests

| Epoxy Networks | $T_g(^{\circ}\text{C})$ | E_f (GPa) | σ_f (MPa) | ϵ_f (%) |
|----------------|-------------------------|-----------------|------------------|------------------|
| DGEG/3DCM | 78.2 | 2.67 ± 0.06 | 87.67 ± 1.03 | 3.65 ± 0.17 |
| DGEG/IPD | 65.5 | 2.32 ± 0.09 | 72.67 ± 1.04 | 3.14 ± 0.19 |
| DGEG/D230 | 12.6 | 0.02 ± 0.01 | - | - |

E_f = Flexural modulus; σ_f , ϵ_f = flexural stress, strain at the maximum.

Table 6. Thermal and mechanical properties of the epoxy networks in compression tests

| Epoxy Networks | $T_g(^{\circ}\text{C})$ | σ_c (MPa) | ϵ_c (%) | ϵ_f (%) |
|----------------|-------------------------|------------------|------------------|------------------|
| DGEG/3DCM | 78.2 | 82.87 ± 0.38 | 6.30 ± 0.29 | 45.71 ± 0.37 |
| DGEG/IPD | 65.5 | 75.40 ± 0.43 | 7.91 ± 0.75 | 57.41 ± 0.51 |
| DGEG/D230 | 12.6 | 8.04 ± 0.04 | 25.01 ± 0.89 | 67.41 ± 0.51 |

σ_c , ϵ_c and ϵ_f = compression yield stress, yield strain and yield strain at the maximum.

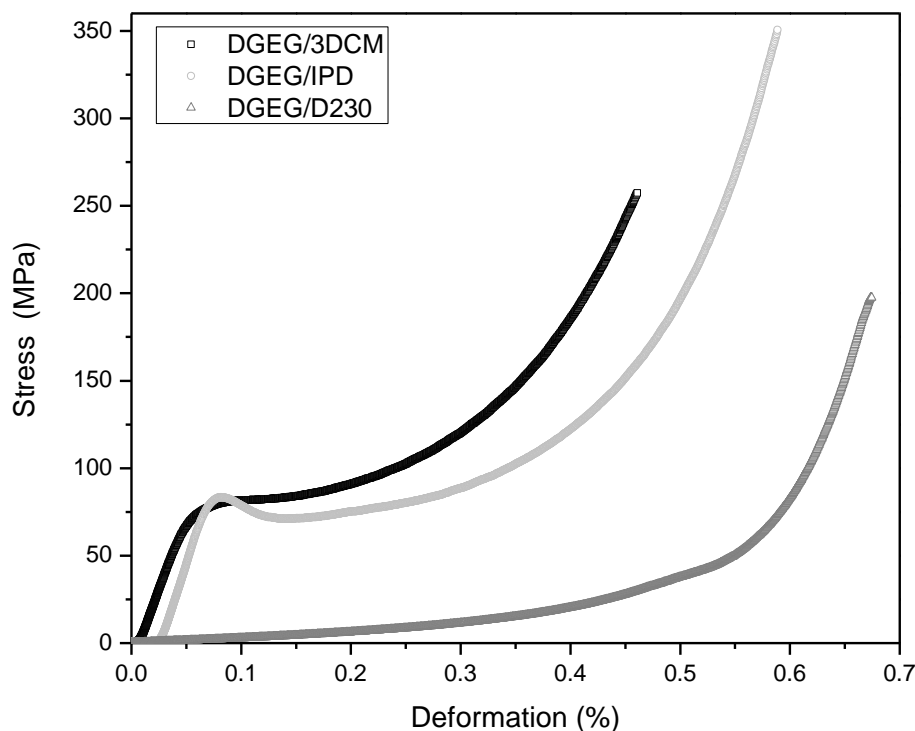


Fig. 5. Typical stress-strain plots for the polymers in compression tests. DGEG/3DCM (black line), DGEG/IPD (LT gray line) and DGEG/D230 (gray line).

The adhesive properties of the different epoxy systems were evaluated in terms single-lap shear using 316L stainless steel which was clean and chemically treated. Table 7 compares the T_g values and the adhesive properties for the three epoxy formulations. The T_g of the epoxy adhesives also presents large influence on the adhesive strength. The systems with relative higher- T_g value (cyclic amines) displayed better adhesive strength.

Table 7. Thermal and adhesive properties of the epoxy networks from single-lap shear tests

| Formulations | T_g (°C) | Adhesive strength in lap shear joints (MPa) |
|--------------|------------|---|
| DGEG/3DCM | 78.2 | 16.36 ± 0.85 |
| DGEG/IPD | 65.5 | 18.06 ± 0.83 |
| DGEG/D230 | 12.6 | 8.91 ± 0.53 |

In this case for a proper interpretation of the relationship between lap-shear strength and T_g value it is important to compare the T_g of the systems with those reported for other epoxy/amine systems (González Garcia F. et al., 2007 and 2010, Pascault J.P. et al., 2002). In this way, the systems with cyclic amines showed lower- T_g values, and the system with the linear amine showed a much lower- T_g value. Therefore, the systems with cyclic amines is in agreement with the relationships between the increased the lap-shear strength with a low- T_g value (González Garcia, F. et al., 2011, Hu X. et al., 2005); but the system with D230 does not meet the relationship. To explain this particular behavior was evaluated the influence of participation of cohesive fracture mechanisms in the lap-shear joints. This information was obtained by analysis of different failures types in the adhesive joints by optical microscopy.

3.3 The failure mechanisms

Different failures types in the adhesive joints can be occur. Failure can occur inside the adhesive layer (cohesive failure with adhesive residues on both surfaces) or at the interface between the adhesive layer and the adherend surface (adhesive failure). The images of the joints after fracture reveal dark and clear regions, corresponding to adhesive and stainless steel surface, respectively. The prevalence of each surface type is shown numerically in Table 8. As can be seen, the cohesive fracture mechanisms have limited participation in the adhesive based on linear diamine D230. However, the adhesive based on cyclic diamine series 3DCM and IPD showed greater participation of cohesive fracture mechanisms. Thus it can be say that the cohesive fracture mechanisms (percentage of cohesive area) significant influence on increased the lap-shear strength (Sampaio E.M. et al., 2006, Prolongo S.G. et al., 2006).

Table 8. Percentage of cohesive failure in the fractured joints with different epoxy adhesive

| Adhesive | Cohesive failure (%) |
|-----------|----------------------|
| DGEG/3DCM | 94 |
| DGEG/IPD | 92 |
| DGEG/D230 | 65 |

3.4 Water absorption

Solvent transport in organic polymer matrices is usually depicted as occurring by a two-step mechanism. In the first step, the solvent dissolves in the superficial polymer layer. This process, which can be considered to occur virtually instantaneously with water as investigated here, creates a concentration gradient. In the second step, the solvent diffuses in the direction of the concentration gradient. This process is described by

the differential mass balance expressed in Fick's second law (Pascault J.P. et al., 2002, Apostol T.M. 1974),^(42,51) which may be written for a one-dimensional case as:

$$\frac{\Delta C_t}{\partial t} = D \frac{\partial^2 C_t}{\partial x^2} \quad (5)$$

where: D is the diffusion coefficient and x the coordinate along the sample's thickness L . For a membrane-shape sample (Apostol T.M. 1974), the resolution of this differential equation is expressed as:

$$\frac{C_t}{C_\infty} = 1 - \sum_{n=0}^{\infty} \frac{8}{(2n+1)^2 \pi^2} \exp \left[\left(\frac{-D(n+1/2)^2 \pi^2 t}{L^2} \right) \right] \quad (6)$$

At short times frames, typically when $C \leq 0.5 C_\infty$, this function can be well approximated by:

$$\frac{C_t}{C_\infty} = 1 - \frac{8}{\pi^2} e^{\left(\frac{-D\pi^2 t}{4L^2} \right)} \quad (7)$$

$$D = \frac{\pi}{16} L^2 \frac{\Delta(C_t/C_\infty)}{\Delta(\sqrt{t})} \quad (8)$$

where: C_t is the mass of water absorbed at time t , C_∞ is the amount of water absorbed at saturation, L is the thickness of the free-standing specimen, and D is the diffusion coefficient.

It is usual to plot $\ln(1 - C_t/C_\infty)$ versus $\ln t$. The linearity of the curve at small $\ln t$ is considered a validity criterion for the application of Fick's second law. The slope of the linear portion allows the determination of the diffusion coefficient (D). To obtain the diffusion time (t_D), the weight gain (%) is plotted over time ($h^{1/2}$). In this plot, t_D is defined as the duration of the transient, can be taken at the intersection of the tangent at the origin and the asymptote. C_∞ was considered the maximum value of the weight gain of the sample. This point corresponds to the value at which the absorption stabilizes.

Figure 6 shows the experimental data for the weight gain over time. All epoxy polymers show linear relationships between the weight gain and the immersion time initially. This behavior is well described by Eq. (8), showing that the initial stage of water absorption behavior is governed by Fick's second law. Therefore, the water concentration gradient drives water absorption in these epoxy polymers. As seen in Figure 6 that the immersion time used caused saturation in all samples.

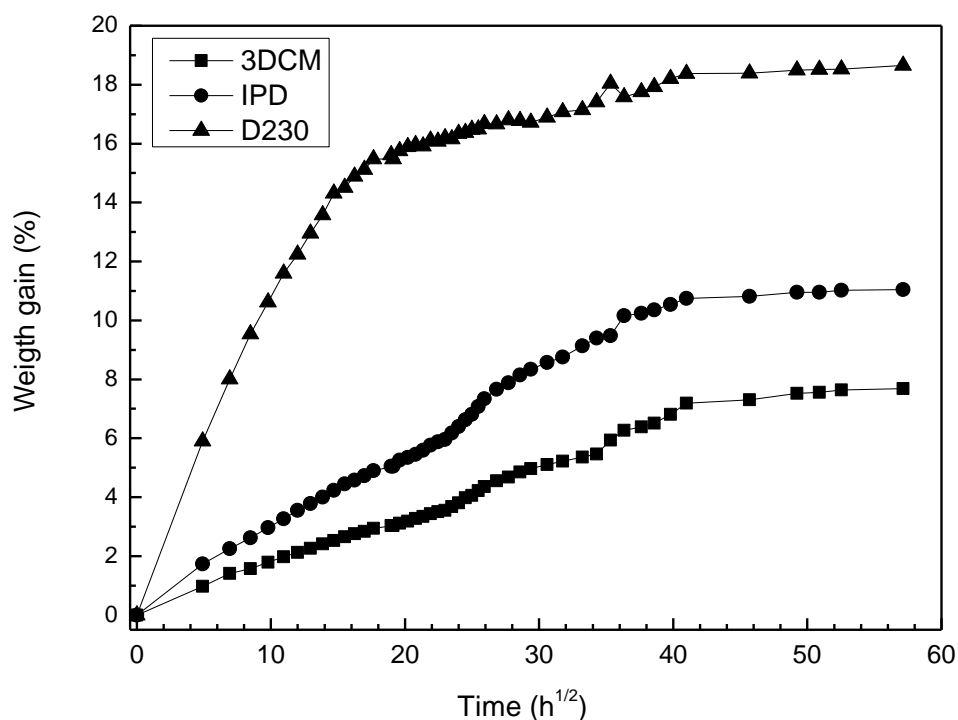


Fig. 6. The gain weight vs. time curve showing the water sorption behavior of the different epoxy adhesives. DGEG/3DCM (■), DGEG/IPD (●) and DGEG/D230 (▲).

The obtained values for C_{∞} , D and t_D are listed in Table 9. Notably, the obtained D is consistent with the values cited for other epoxy polymers (Berry N.G. et al., 2007, Pascault J.P. et al., 2002, Maggana C. et al., 1999, Moy, P. et al., 1980). C_{∞} , D and t_D change for each epoxy network depending on the diamine as curing agents employed. C_{∞} and D for the linear diamine D230 are always higher than those of the series based on cyclic diamines and t_D is the smallest for all the networks. The series based on cyclic amines (3DCM and IPD) exhibit similar C_{∞} . However the D and t_D values do not follow the same behavior. In this case, the cyclic amine 3DCM present higher values compared with cyclic amine IPD. This may be related with the molecular structure of these compounds.

Table 9. Diffusion coefficient (D , m²/s), saturation value (C_{∞} , %) and diffusion time t_D , days) obtained from experimental weight gain vs. time curve of DGEG/3DCM, DGEG/IPD and DGEG/D230 systems.

| oxy networks | DGEG/3DCM | DGEG/IPD | DGEG/D230 |
|---------------------------|-----------|----------|-----------|
| C_{∞} (%) | 1.711 | 1.782 | 1.870 |
| D (x10 ⁻¹²) | 0.929 | 0.455 | 7.752 |
| t_D (days) | 74.41 | 5.86 | 9.28 |

Some authors suggest that the diffusion kinetics, in aliphatic diepoxide cured by aromatic diamine, the diffusion rate of water is controlled by the presence of strong hydrogen bonds between water molecules and the polar groups (essentially hydroxyls) of the polymer (Tcharkhtchi, A. et al., 2000). On the other hands, others authors support that the molecular structures of the diamines and the degree of crosslinking affect the water absorption (Abdelkader A.F. et al., 2005). Nevertheless, the structure-diffusivity relationships have not clearly established. Considering these factors the series based on cyclic (3DCM and IPD) and linear

diamine (D230) the polar groups (essentially hydroxyls) concentration may be disregarded; but the molecular structure of the aliphatic diamine D230 has a linear and have a greater mobility between elastically active chains spacing (flexibility) and this may be improve the diffusion rate of water. In particular for the series based on cyclic diamines 3DCM and IPD the first diamine has a more rigid molecular structure than the latter diamine, decreasing D and t_D values. In this case, can be more complicates to explain the diffusion rate of water. However, our results indicate that the diffusion rate of water decrease with increase of the rigidity of the molecular structure of the curing agent.

4. CONCLUSIONS

The dynamical mechanical behavior, mechanical properties, adhesive strength in terms single lap-shear using 316L stainless steel as the adherend and water absorption of the tested epoxy networks are compared with the chemical structures of linear and cyclic aliphatic diamine used as comonomer, which change the structures of the epoxy networks. The polymers based on cyclic diamines showed relative higher- T_g values, greater compression, yield stress and the best adhesive strength compared with the polymer based on linear diamine. Nevertheless, the polymer based on linear diamine shows the best flexibility, but poor adhesive strength, and higher water absorption. Finally, was demonstrating that the cohesive fracture mechanisms increased the lap-shear strength and the diffusion rate of water decreased with increasing with the rigidity of the molecular structure of the curing agent.

5. REFERENCES

- Abadyan, M., Bagheri, R., & Kouchakzadeh, M.A. (2012) Fracture toughness of a hybrid-rubber-modified epoxy. I. Synergistic toughening. *Journal of Applied Polymer Science*, 125(3), 2467-2475.
- Abdelkader, A.F., & While, J.R. (2005) Water absorption in epoxy resins: The effects of the crosslinking agent and curing temperature. *Journal of Applied Polymer Science*, 98(6), 2544-2549.
- Apostol, T.M. (1973). *Mathematic Analysis*. United States of America: Addison-Wesley Publishing Company.
- Berry, N.G., de Almeida, J.R., Barcia, F.L., & Soares, B.G. (2007) Effect of water absorption on the thermal-mechanical properties of HTPB modified DGEBA-based epoxy systems. *Polymer Testing*, 26(2), 262-267.
- Cai, H., Li, P., Sui, G., Yu, H., Li, G., Yian, X., & Ryu, S. (2008) Curing kinetics study of epoxy resin/flexible amine toughness systems by dynamic and isothermal DSC. *Thermochimica Acta*, 473(1-2), 101-105.
- Chang, T.D., Carr, S.H., & Brittain, J.O. (1982) Studies of epoxy resin systems: Part B: Effect of crosslinking on the physical properties of an epoxy resin. *Polymer Engineering Science*, 22(18), 1213-1220.
- Charlesworth, J.M. (1988) Effect of crosslink density on the molecular relaxations in diepoxide-diamine network polymers. Part 1. The glassy region. *Polymer Engineering Science*, 28(4), 221-229.

Chovelon, J.M., Aarch, L.E.L., Charbonnier, M., & Romand, M. (1995) Silanization of stainless steel surfaces: Influence of application parameters. *Journal of Adhesion*, 50(1), 43-58.

Choy, I. C., & Plazek, D.J. (1986) The physical properties of bisphenol-A-based epoxy resins during and after curing. *Journal of Polymer Science Part B: Polymer Physics*, 24(6), 1303-1320.

Cizmecioglu, M., Gupta, A., & Fedors, R.F. (1986) Influence of cure conditions on glass transition temperature and density of an epoxy resin. *Journal Applied Polymer Science*, 32(8), 6177-6190.

Colombini, D., Martinez-Vega, J.J., & Merle, G. (2002) Dynamic mechanical investigations of the effects of water sorption and physical ageing on an epoxy resin system. *Polymer*, 43(16), (2002) 4479-4485.

Cook, W.D., Mayr A.E. & Edward, G.H. (1998) Yielding behavior in model epoxy thermosets - II. Temperature dependence. *Polymer*, 39(16), 3725-3733.

Crawford, E.D., & Lesser, A.J. (1999) Brittle to ductile: Fracture toughness mapping on controlled epoxy networks. *Polymer Engineering Science*, 39(2), 385-392.

Cukierman, S., Halary, J.L., & Monnerie, L. (1991) Molecular analysis of the viscoelastic properties of epoxy networks as deduced from the study of model systems. *Journal of Non-Crystalline Solids*, 131-133(2), 898-905.

De Morais, A.B., Pereira, A.B., Teixeira, J.P., & Cavaleiro, N.C. (2007) Strength of epoxy adhesive-bonded stainless-steel joints. *International Journal of Adhesion and Adhesives*, 27(March), 679-686.

Delvigs P. (1986) Tetraglycidyl epoxy resins and graphite fiber composites cured with flexibilized aromatic diamines. *Polymer Composites*, 7(2), 101-105.

Fernandez-Nogro, F., Valea, A., Llanto-Ponte, R., & Mondragon, I. (1996) Dynamic and mechanical properties of DGEBA/poly(propylene oxide) amine based epoxy resins as a function of stoichiometry. *European Polymer Journal*. 32(2), 257-266.

Froimowicz, P., Gandini, A., & Strumia, M. (2005) New polyfunctional dendritic linear hybrids from terminal amine polyether oligomers (Jeffamine®): synthesis and characterization. *Tetrahedron Letters*, 46(15), 2653-2657.

González Garcia, F., da Silva, P.M., Soares, B.G., & Rieumont, J (2007) Combined analytical techniques for the determination of the amine hydrogen equivalent weight in aliphatic amine epoxide hardeners. *Polymer Testing*, 26(1), 95-101.

González Garcia, F., de Queiroz, A.A.A., Higa, O.Z., & Baratéla F.J.C. Epoxy polymers: Biocompatible properties related to chemical structure of comonomer. *Journal of Biomaterials Applications* (Submit in 2017).

González Garcia, F., Leyva, M.E., de Queiroz, A.A.A., & Higa, O.Z. (2009) Epoxy networks for medicine applications: Mechanical properties and in vitro biological properties. *Journal of Applied Polymer Science*, 112(3), 1215-1225.

González Garcia, F., Leyva, M.E., de Queiroz, A.A.A., & Simões, A.Z. (2011) Durability of adhesives based on different epoxy/aliphatic amine networks. *International Journal of Adhesion and Adhesives*. 31(4), 177-181.

González Garcia, F., Leyva, M.E., Oliveira, M.G., de Queiroz, A.A.A., & Simões, A. Z. (2010) Influence of chemical structure of hardener on mechanical and adhesive properties of epoxy polymers. *Journal of Applied Polymer Science*, 117(4), 2213-2219.

González Garcia, F., Soares, B.G., Leyva, M.E. & Simões, A.Z. (2010) Influence of aliphatic amine epoxy hardener on the adhesive properties of blends of mono-carboxyl-terminated poly(2-ethylhexyl acrylate-co-methyl methacrylate) with epoxy resin. *Journal of Applied Polymer Science*, 117(5), 2762-2770.

González Garcia, F., Soares, B.G., Pita, V.J.R.R., Sánchez, R., & Rieumont, J. (2007) Mechanical properties of epoxy networks based on DGEBA and aliphatic amines. *Journal of Applied Polymer Science*, 106(3), 2047-2055.

González Garcia, F., Vicente, Thiago A., de Queiroz, A.A.A., Higa, O.Z., & Baratéla, F.J.C. (2016) Epoxy/aliphatic amine networks with perspectives for cardiovascular applications. In vitro biological properties. *Revista Matéria*, 21(1), 115-118.

Grillet, A.C., Galy, J., & Pascault, J.P. (1989) Effects of the structure of the aromatic curing agent on the cure kinetics of epoxy networks. *Polymer*, 30(11), 2094-2103.

Heux, L., Halary, J.L., Lauprêtre, F. & Monnerie, L. (1997) Dynamic mechanical and ¹³C n.m.r. investigations of molecular motions involved in the β relaxation of epoxy networks based on DGEBA and aliphatic amines. *Polymer*, 38(8), 1767-1778.

Hu, X., & Huang, P. (2005) Influence of polyether chain and synergetic effect of mixed resins with different functionality on adhesion properties of epoxy adhesives. *International Journal of Adhesion and Adhesives*, 25(4), 296-300.

Khoe, S., & Hassani, N. (2010) Adhesion strength improvement of epoxy resin reinforced with nanoelastomeric copolymer. *Materials Science Engineering: A*, 527(24-25), 6562-6567.

Kuan, H.C., Dai, J.B., & Ma, J. (2010) A reactive polymer for toughening epoxy resin. *Journal of Applied Polymer Science*, 115(3), 3265-3272.

Lapique, F., & Redford, K. (2002) Curing effects on viscosity and mechanical properties of a commercial epoxy resin adhesive. *International Journal of Adhesion and Adhesives*, 22(4), 337-346.

Maggana, C., Pissis, P. (1999). Water sorption and diffusion studies in an epoxy resin system. *J. Polym. Sci: Part B Polym Phys*, 37(11), 1165-1182.

Maiez-Tribu, S., Pascault, J.P., Soulé, E.R., Borrajo, J., & Williams, R.J.J. (2007) Nanostructured epoxies based on the self-assembly of block copolymers: A new miscible block that can be tailored to different epoxy formulations. *Macromolecules*, 40(4), 1268-1273.

Morel, E., Bellenger, V., Bocquet, M., & Verdu J. (1989) Structure-properties relationships for densely cross-linked epoxide-amine systems based on epoxide or amine mixtures. *Journal of Materials Science*, 24(1), 69-75.

Mortarnal, S., Pascault, J.P. Sautereau H. (1989) In *Rubber-Toughened Plastics*, No. 222 Riew C. K., ed., ACS, Washintong, D.C.

Moy, P., & Karasz, F.E. (1980) Epoxy-water interactions. *Polymer Engineering Science*, 20(4), 315-319.

Ochi, M. Yoshizumi, M., & Shimbo, M. (1987) Mechanical and dielectric relaxations of epoxide resins containing the spiro-ring structure. II. Effect of the introduction of methoxy branches on low-temperature relaxations of epoxide resins. *Journal of Polymer Science Part B: Polymer Physics*, 25(9), 1817-1827.

Ochi, M., Iesako, H., & Nakajima, S. (1986) Mechanical relaxation mechanism of epoxide resins cured with acid anhydrides. II. Effect of the chemical structure of the anhydrides on the β relaxation mechanism. *Journal of Polymer Science Part B: Polymer Physics*, 24(2), 251-261.

Ochi, M., Lesako, H., & Shimbo, M. (1985) Mechanical relaxation mechanism of epoxide resins cured with diamines. *Polymer*, 26(3), 457-461.

Ochi, M., Shimbo, M., Saga, M. & Takashima, N. (1986) Mechanical and dielectric relaxations of epoxide resins containing spiro-ring structure. *Journal of Polymer Science Part B Polymer Physics*, 24(10), 2185-2195.

Omrani, A., Rostami, A.A., Ravari, F., & Mashak, A. (2011) Curing behavior and structure of a novel nanocomposite from glycerol diglycidyl ether and 3,3-dimethylglutaric anhydride. *Thermochimica Acta*, 517(1-2), 9-15.

Omrani, A., Rostami, A., Ravari, F., & Ehsani, M. (2013) The relationship between composition and electrical properties of brass covered by a nanocomposite coating of glycerol diglycidyl ether: An EIS and DMTA study. *Progress in Organic Coating*, 76(2-3), 360-366.

Pascault, J.P., Sautereau, H., Verdu, J., & Williams R.J.J. (2002) *Thermosetting Polymers*. New York: Marcel Dekker. (ISBN: 0-8247-0670-6).

Pineda, A.F.E., González Garcia, F., Simões, A.Z., & da Silva, E.L. (2016) Mechanical properties, water absorption and adhesive properties of diepoxy aliphatic diluent-modified DGEBA/Cycloaliphatic amine networks on 316 L stainless steel. *International Journal of Adhesion and Adhesives*, 68(July), 205-211.

Prolongo, S.G., Rosario, G., & Ureña, A. (2006) Comparative study on the adhesive properties of different epoxy resins. *International Journal of Adhesion and Adhesives*, 26(3), 125-132.

Sampaio, E.M., González Garcia, F., Limaverde, A.M., Perrut, P.A. Aderência de juntas metálicas de cisalhamento coladas com adesivos epoxídicos de baixa e alta viscosidade. In *Anais do 17º CBECIMat; Congresso Brasileiro de Engenharia e Ciência dos Materiais, Foz de Iguaçu - Paraná, novembro (2006), Brazil*.

Silva, A.C.F., Ortega, P.P., González Garcia, F., de Queiroz, A.A.A., Higa, O.Z., Baratéla, F.J.C., & Simões, A.Z. (2016) Propiedades biológicas in vitro de polímeros modificados con diluyente reactivo. *Revista Iberoamericana de Polímeros*, 17(5), 231-246.

Struik, L.C.E. (1987) Effect of thermal history on secondary relaxation processes in amorphous polymers. *Polymer*, 28(1), 57-68.

Tcharkhtchi, A., Bronnec, P.Y., & Verdu, J. (2000) Water absorption characteristics of diglycidylether of butane diol-3,5-diethyl-2,4-diaminotoluene networks. *Polymer*, 41(15), 5777-5785.

Tripathy, R., Ojha, U., & Faust, R. (2011) Polyisobutylene modified bisphenol A diglycidyl ether based epoxy resins possessing improved mechanical properties. *Macromolecules*, 44(17), 6800-6809.

Urbaczewski-Espuche, E., Galy, J., Gérard, J.F., Pascault, J.P. & Sautereau, H. (1991) Influence of chain flexibility and crosslink density on mechanical properties of epoxy/amine networks. *Polymer Engineering Science*, 31(22), 1572-1580.

Varma, I. F., & Satya-Bhama P.V. (1986) Epoxy resins: Effect of amines on curing characteristics and properties. *Journal of Composite Materials*, 20(5), 410-422.

Won, Y.G., Galy, J., Gerard, J.F., Pascault, J.P., & Bellenger, V., & Verdu, J. (1990) Internal antiplasticization in copolymer and terpolymer networks based on diepoxides, diamines and monoamines. *Polymer*, 31(9), 1787-1792.

Yan, G., Fu, S.Y., & Yan, J.P. (2007) Preparation and mechanical properties of modified epoxy resins with flexible diamines. *Polymer*, 48(1), 302-310.